

Orbital periods of cataclysmic variables identified by the SDSS.

IX. NTT photometry of eight eclipsing and three magnetic systems

John Southworth¹, C. Tappert², B. T. Gänsicke³, and C. M. Copperwheat⁴

¹ Astrophysics Group, Keele University, Staffordshire, ST5 5BG, UK e-mail: astro.js@keele.ac.uk

² Instituto de Astronomía y Astrofísica, Pontificia Universidad Católica, Av. Vicuña Mackenna 4860, 782-0436 Macul, Santiago, Chile

³ Department of Physics, University of Warwick, Coventry, CV4 7AL, UK

⁴ Astrophysics Research Institute, Liverpool John Moores University, Liverpool, L3 5RF, UK

Received 2014/09/26; accepted 2014/11/10

ABSTRACT

We report the discovery of eclipses and the first orbital period measurements for four cataclysmic variables, plus the first orbital period measurements for one known eclipsing and two magnetic systems. SDSS J093537.46+161950.8 exhibits 1-mag deep eclipses with a period of 92.245 min. SDSS J105754.25+275947.5 has short and deep eclipses and an orbital period of 90.44 min. Its light curve has no trace of a bright spot and its spectrum is dominated by the white dwarf component, suggesting a low mass accretion rate and a very low-mass and cool secondary star. CSS J132536+210037 shows 1-mag deep eclipses each separated by 89.821 min. SDSS J075653.11+085831.8 shows 2-mag deep eclipses on a period of 197.154 min. CSS J112634–100210 is an eclipsing dwarf nova identified in the *Catalina Real Time Transit Survey*, for which we measure a period of 111.523 min. SDSS J092122.84+203857.1 is a magnetic system with an orbital period of 84.240 min; its light curve is a textbook example of cyclotron beaming. A period of 158.72 min is found for the faint magnetic system SDSS J132411.57+032050.4, whose orbital light variations are reminiscent of AM Her. Improved orbital period measurements are also given for three known SDSS cataclysmic variables. We investigate the orbital period distribution and fraction of eclipsing systems within the SDSS sample and for all cataclysmic variables with a known orbital period, with the finding that the fraction of known CVs which are eclipsing is not strongly dependent on the orbital period.

Key words. stars: dwarf novae — stars: novae, cataclysmic variables – stars: binaries: eclipsing – stars: binaries: spectroscopic – stars: white dwarfs

1. Introduction

Cataclysmic variables (CVs) are interacting binary stars composed of a white dwarf orbited by a low-mass secondary star which fills its Roche lobe. In most CVs the secondary star is hydrogen-rich and loses material to the white dwarf via an accretion disc. Comprehensive reviews on the subject of CVs have been given by Warner (1995) and Hellier (2001). Their evolution is dominated by the loss of orbital angular momentum, which results in CVs evolving from longer orbital periods down to a period minimum, caused by the changes in the structure of the mass donor, before turing back to longer periods. This evolutionary process leaves a strong imprint on the orbital period distribution of the known CV population, which is discussed in detail by Gänsicke et al. (2009).

The optical light of most CVs is dominated by continuum emission and broad emission lines arising from the accretion disc. This swamps the spectral signatures of the white dwarf and secondary star, making it very difficult to characterise the physical properties of these components. Particularly for short-period CVs, the mass donor is often only detectable if it occults the white dwarf and accretion disc. Eclipsing CVs are therefore a valuable resource, as analysis of the eclipse shapes is one of the few ways of revealing the masses and radii of all three components of the system (Wood et al. 1989; Horne et al. 1991; Littlefair et al. 2006, 2008).

A fraction of CVs harbour magnetic white dwarfs, and these objects have quite different evolutionary processes to the non-

magnetic CVs (Webbink & Wickramasinghe 2002; Norton et al. 2004). If the white dwarf's magnetic field is sufficiently strong it disrupts the accretion disc, and accretion occurs along the field lines to the magnetic poles on the white dwarf surface. Interaction between the magnetic fields of the white dwarf and the mass donor also suppresses or reduces the efficiency of magnetic braking (Araujo-Betancor et al. 2005). The interplay of plasmas with strong magnetic fields makes these objects natural laboratories for physics in extreme environments.

We are engaged in characterising the population of CVs spectroscopically identified by the Sloan Digital Sky Survey (SDSS¹; see Szkody et al. 2011 and references therein). Our primary aim is to measure the orbital periods of these objects; further information and previous results can be found in Gänsicke et al. (2006), Dillon et al. (2008) and Southworth et al. (2006, 2007a). Detecting eclipses is one of the most reliable and straightforward ways of measuring the orbital period of a CV. Similarly, magnetic CVs tend to be highly variable in brightness due to processes such as cyclotron emission. In this work we present photometry of eleven objects and measure precise orbital periods for ten of these systems. Basic information for all the objects observed is compiled in Table 1, which contains the abbreviated names which we will use throughout this paper. The SDSS spectra for six of these objects are reproduced in Fig. 1 for reference.

¹ <http://www.sdss.org/>

Table 1. Full and abbreviated names, references and SDSS apparent *ugriz* magnitudes of the targets.

SDSS name	Short name	Reference	<i>u</i>	<i>g</i>	<i>r</i>	<i>i</i>	<i>z</i>	<i>g_{spec}</i>
SDSS J075059.97+141150.1	SDSS J0750	Szkody et al. (2007)	19.20	19.09	18.98	18.79	18.58	18.83
SDSS J075653.11+085831.8	SDSS J0756	Szkody et al. (2011)	16.70	16.25	16.29	16.34	16.38	17.27
SDSS J092122.84+203857.1	SDSS J0921	Szkody et al. (2009)	20.68	19.85	19.16	19.17	19.64	19.20
SDSS J092444.48+080150.9	SDSS J0924	Szkody et al. (2005)	19.49	19.25	19.26	18.70	17.88	19.36
SDSS J093537.46+161950.8	SDSS J0935	Szkody et al. (2009)	19.51	19.08	18.99	19.01	18.99	18.77
SDSS J100658.40+233724.4	SDSS J1006	Southworth et al. (2009a)	18.46	18.31	17.93	17.51	17.14	18.63
SDSS J105754.25+275947.5	SDSS J1057	Szkody et al. (2009)	19.87	19.61	19.61	19.81	19.65	19.64
CSS J112634-100210	CSS J1126	Drake et al. (2009)	18.81	18.81	18.61	18.38	18.12	
SDSS J132411.57+032050.4	SDSS J1324	Szkody et al. (2004)	23.74	22.08	20.46	20.19	19.42	23.29
CSS J132536+210037	CSS J1325	Wils et al. (2010)	21.94	23.10	20.38	20.63	20.55	
SDSS J133309.19+143706.9	SDSS J1333	Szkody et al. (2009)	19.11	18.48	18.15	17.94	17.90	20.95

Notes. *g_{spec}* is a spectroscopic apparent magnitude calculated by convolving the SDSS flux-calibrated spectra with the *g*-band response function. These correspond to a different epoch to the photometric magnitudes, but may be affected by ‘slit losses’ due to errors in astrometry or fibre positioning.

Table 2. Log of the observations presented in this work. The mean magnitudes are calculated using only observations outside eclipses. The dates are for the first observation in that observing sequence. The start and end times indicate the beginning of the first and last exposures in the observing sequence.

Target	Date of first observation (UT)	Start time (UT)	End time (UT)	Telescope/instrument	Optical element	Number of observations	Exposure time (s)	Mean magnitude
SDSS J0750	2010 02 24	00:27	01:10	NTT/EFOSC2	<i>B_{Tyson}</i> filter	18	30–60	19.3
SDSS J0756	2010 02 27	00:47	03:38	NTT/EFOSC2	<i>B_{Tyson}</i> filter	65	60	17.6
SDSS J0756	2010 02 27	05:01	05:30	NTT/EFOSC2	<i>B_{Tyson}</i> filter	13	60	17.5
SDSS J0756	2010 02 28	00:25	03:38	NTT/EFOSC2	<i>B_{Tyson}</i> filter	96	30	17.6
SDSS J0921	2009 01 22	05:32	09:08	NTT/EFOSC2	<i>B_{Tyson}</i> filter	162	40–80	20.5
SDSS J0921	2009 01 23	03:42	05:31	NTT/EFOSC2	<i>B_{Tyson}</i> filter	89	40	20.5
SDSS J0921	2009 01 23	07:37	09:06	NTT/EFOSC2	<i>B_{Tyson}</i> filter	70	40–80	20.5
SDSS J0921	2009 01 27	03:33	05:00	NTT/EFOSC2	<i>B_{Tyson}</i> filter	71	40	20.5
SDSS J0924	2010 02 26	00:16	01:42	NTT/EFOSC2	<i>B_{Tyson}</i> filter	18	180–240	19.6
SDSS J0935	2010 02 24	01:19	05:07	NTT/EFOSC2	<i>B_{Tyson}</i> filter	56	90–180	19.0
SDSS J0935	2010 02 25	04:32	05:37	NTT/EFOSC2	<i>B_{Tyson}</i> filter	21	90–120	18.8
SDSS J0935	2010 03 01	03:25	04:48	NTT/EFOSC2	<i>B_{Tyson}</i> filter	29	90	19.0
SDSS J1006	2010 03 01	04:59	05:44	NTT/EFOSC2	<i>B_{Tyson}</i> filter	11	180	18.5
SDSS J1057	2010 02 26	03:26	06:30	NTT/EFOSC2	<i>B_{Tyson}</i> filter	29	300	19.5
SDSS J1057	2010 02 27	03:42	04:52	NTT/EFOSC2	<i>B_{Tyson}</i> filter	15	210	19.5
SDSS J1057	2010 03 01	05:54	06:54	NTT/EFOSC2	<i>B_{Tyson}</i> filter	13	210	19.4
CSS J1126	2010 02 26	02:07	02:51	NTT/EFOSC2	<i>B_{Tyson}</i> filter	11	180	18.5
CSS J1126	2010 02 26	06:51	07:33	NTT/EFOSC2	<i>B_{Tyson}</i> filter	13	120	18.5
CSS J1126	2010 02 26	08:41	09:33	NTT/EFOSC2	<i>B_{Tyson}</i> filter	16	120	18.4
CSS J1126	2010 02 27	05:34	06:10	NTT/EFOSC2	<i>B_{Tyson}</i> filter	11	120	18.3
CSS J1126	2010 03 01	07:07	08:16	NTT/EFOSC2	<i>B_{Tyson}</i> filter	21	120	18.2
SDSS J1324	2009 01 25	07:35	09:13	NTT/EFOSC2	<i>B_{Tyson}</i> filter	63	60	21.1
SDSS J1324	2009 01 26	05:26	09:11	NTT/EFOSC2	<i>B_{Tyson}</i> filter	144	60	21.1
SDSS J1324	2009 01 27	05:40	09:12	NTT/EFOSC2	<i>B_{Tyson}</i> filter	111	80	21.1
CSS J1325	2010 02 25	06:17	09:24	NTT/EFOSC2	<i>B_{Tyson}</i> filter	30	240–300	19.8
CSS J1325	2010 02 26	07:39	08:34	NTT/EFOSC2	<i>B_{Tyson}</i> filter	11	240	19.9
CSS J1325	2010 02 27	07:22	07:54	NTT/EFOSC2	Grism #11	3	900	
CSS J1325	2010 03 01	08:24	09:36	NTT/EFOSC2	<i>B_{Tyson}</i> filter	14	240	20.1
SDSS J1333	2010 02 27	06:20	06:36	NTT/EFOSC2	<i>B_{Tyson}</i> filter	4	180–240	19.7
SDSS J1333	2010 02 27	07:02	07:07	NTT/EFOSC2	<i>B_{Tyson}</i> filter	2	240	18.9
SDSS J1333	2010 02 27	08:13	09:45	NTT/EFOSC2	<i>B_{Tyson}</i> filter	18	240	19.3
SDSS J1333	2010 02 28	07:52	09:42	NTT/EFOSC2	<i>B_{Tyson}</i> filter	21	210–240	19.5
SDSS J1333	2010 05 12	23:58	02:30	CA35/LAICA	<i>g</i> filter	145	60	19.4

2. Observations and data reduction

with the EFOSC2 focal-reducing instrument² (Buzzoni et al. 1984). EFOSC2 was used in imaging mode with a Loral 2048×2048 px² CCD, giving a field of view of 4.4×4.4 arcmin² at a plate scale of 0.13'' px⁻¹. For the 2009 observing run we

The observations presented in this work were obtained using the New Technology Telescope (NTT) at ESO La Silla, equipped

² <http://www.eso.org/sci/facilities/lasilla/instruments/efosc/index.html>

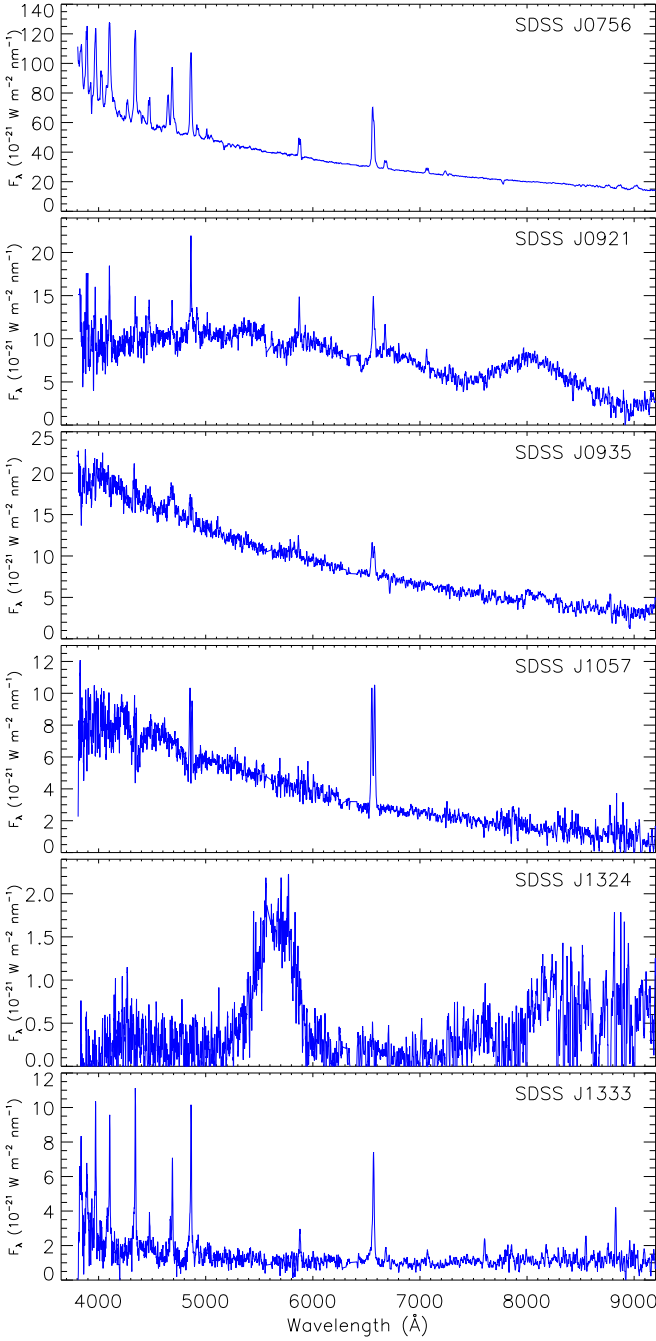


Fig. 1. SDSS spectra of six of the CVs for which we provide the first precise orbital period measurement (CSS J1126 and CSS J1325 have not been observed spectroscopically by the SDSS). The flux levels have been smoothed with 10-pixel Savitsky-Golay filters for display purposes. The units of the abscissae are $10^{-21} \text{ W m}^{-2} \text{ nm}^{-1}$, which corresponds to $10^{-17} \text{ erg s}^{-1} \text{ cm}^{-2} \text{ Å}^{-1}$.

binned the CCD 2×2 , but for the 2010 run the CCD was unbinned. All NTT images were obtained with a B_{Tyson} filter (ESO filter #724), which has a central wavelength of 4445 Å and a FWHM of 1838 Å .

A few additional observations of SDSS J1333 were obtained on the night of 2010/05/12, in poor seeing conditions, and using the Calar Alto 3.5 m telescope and LAICA wide-area camera.

The CCD was binned 4×4 , yielding an effective plate scale of $1.0'' \text{ px}^{-1}$, and images of duration 60 s were obtained through a Gunn g filter.

All data were reduced using the DEFOT pipeline, written in IDL³ (Southworth et al. 2009b, 2014). Aperture photometry was performed using the ASTROLIB/APER procedure⁴, which originates from DAOPHOT (Stetson 1987).

The instrumental differential magnitudes were transformed to apparent V magnitudes using formulae from Jordi et al. (2006) and SDSS magnitudes of the comparison stars. Given the variety of spectral energy distributions of CVs, and the response function of B_{Tyson} filter we used, the zeropoints of the apparent magnitudes are uncertain by at least several tenths of a magnitude.

2.1. Times of minimum light

Eclipse midpoints were measured by shifting each light curve against its own mirror-image until the respective ascending and descending branches were in the best agreement. The time defining the axis of reflection was taken as the midpoint of the eclipse, and uncertainties were estimated based on the shift required for which an offset was obvious. All known times of minimum light for our targets are collected in Table 3.

Due to the poor sky conditions during the 2010 February observing run (bright moon and bad seeing) we had to use rather long exposure times to obtain good photometry of our target objects. Some eclipses were therefore covered by only one datapoint, in which case we quote the midpoint of the exposure and take the uncertainty to be half of the exposure time. This poor sampling rate prevents us from using the data to measure the physical properties of the CVs from modelling their light curves.

The results for each system are presented below in three categories. Firstly we discuss and give the first orbital period measurements of the four new eclipsing CVs. Then we obtain improved ephemerides for four CVs previously known to be eclipsing. Finally, we present light curves obtained for the three magnetic systems SDSS J0921, SDSS J1324 and SDSS J1333.

3. Four new eclipsing cataclysmic variables

3.1. SDSS J075653.11+085831.8

SDSS J0756 was identified as a variable star in a search for new dwarf novae in existing photometric and astrometric catalogues (Wils et al. 2010). Its variability amplitude (1.2 mag between multiple SDSS photometric observations) was below the 1.5 mag minimum value used in that work to identify dwarf novae. However, its SDSS spectrum was inspected and found to be typical of the SW Sex stars, which are the dominant population of CVs in the 3–4 hr orbital period interval. A defining characteristic of SW Sex stars is spectra which feature a hot continuum with strong He II and Bowen blend emission; many of them also show eclipses (Thorstensen et al. 1991; Rodríguez-Gil et al. 2007).

Two complete eclipses of SDSS J0756 were observed on successive nights using the NTT (Fig. 2). On the second of these nights we also obtained a single datapoint which was clearly in

³ The acronym IDL stands for Interactive Data Language and is a trademark of ITT Visual Information Solutions. For further details see <http://www.itervis.com/ProductServices/IDL.aspx>.

⁴ The ASTROLIB subroutine library is distributed by NASA. For further details see <http://idlastro.gsfc.nasa.gov/>.

Table 3. All available measured times of eclipse for the objects studied in this work.

Object	Time of eclipse (HJD(UTC))	Cycle	Residual (d)	Ref.
SDSS J0750	2454853.6293 ± 0.0002	-277.0	0.00016	1
SDSS J0750	2454853.7225 ± 0.0002	-276.0	0.00020	1
SDSS J0750	2454854.5612 ± 0.0003	-267.0	0.00041	1
SDSS J0750	2454857.6353 ± 0.0002	-234.0	0.00005	1
SDSS J0750	2454858.5670 ± 0.0003	-224.0	0.00009	1
SDSS J0750	2454879.4358 ± 0.0001	0.0	-0.00017	1
SDSS J0750	2455251.5388 ± 0.0001	3994.0	0.00001	2
SDSS J0756	2455254.5481 ± 0.0001	0.0	0.00000	2
SDSS J0756	2455255.6434 ± 0.0001	8.0	0.00000	2
SDSS J0924	2454856.7192 ± 0.0002	-250.0	-0.00013	1
SDSS J0924	2454856.8104 ± 0.0003	-249.0	-0.00008	1
SDSS J0924	2454857.7220 ± 0.0002	-239.0	0.00011	1
SDSS J0924	2454858.7245 ± 0.0002	-228.0	0.00006	1
SDSS J0924	2454879.5046 ± 0.0002	0.0	-0.00001	1
SDSS J0924	2455253.5476 ± 0.0014	4104.0	-0.00001	2
SDSS J0935	2455251.5662 ± 0.0004	0.0	-0.00041	2
SDSS J0935	2455251.6309 ± 0.0007	1.0	0.00023	2
SDSS J0935	2455251.6946 ± 0.0004	2.0	-0.00013	2
SDSS J0935	2455252.7203 ± 0.0004	18.0	0.00062	2
SDSS J0935	2455256.6912 ± 0.0004	80.0	-0.00014	2
SDSS J1006	2454497.6338 ± 0.0005	-231.0	0.00015	3
SDSS J1006	2454540.5802 ± 0.0005	0.0	0.00058	3
SDSS J1006	2454541.5091 ± 0.0002	5.0	-0.00009	3
SDSS J1006	2454821.6805 ± 0.0002	1512.0	-0.00004	3
SDSS J1006	2455256.7178 ± 0.0005	3852.0	0.00012	2
SDSS J1057	2455253.6903 ± 0.0017	0.0	-0.00103	2
SDSS J1057	2455253.7555 ± 0.0017	1.0	0.00136	2
SDSS J1057	2455254.6958 ± 0.0017	16.0	-0.00045	2
SDSS J1057	2455256.7690 ± 0.0017	49.0	0.00012	2
CSS J1126	2455253.8126 ± 0.0001	0.0	-0.00008	2
CSS J1126	2455253.8905 ± 0.0002	1.0	0.00037	2
CSS J1126	2455254.7420 ± 0.0002	12.0	-0.00004	2
CSS J1126	2455256.8331 ± 0.0001	39.0	0.00000	2
CSS J1325	2455252.7705 ± 0.0005	-1.0	-0.00034	2
CSS J1325	2455252.8332 ± 0.0001	0.0	-0.00002	2
CSS J1325	2455252.8954 ± 0.0003	1.0	-0.00019	2
CSS J1325	2455253.8313 ± 0.0001	16.0	0.00007	2
CSS J1325	2455256.8872 ± 0.0005	65.0	-0.00044	2

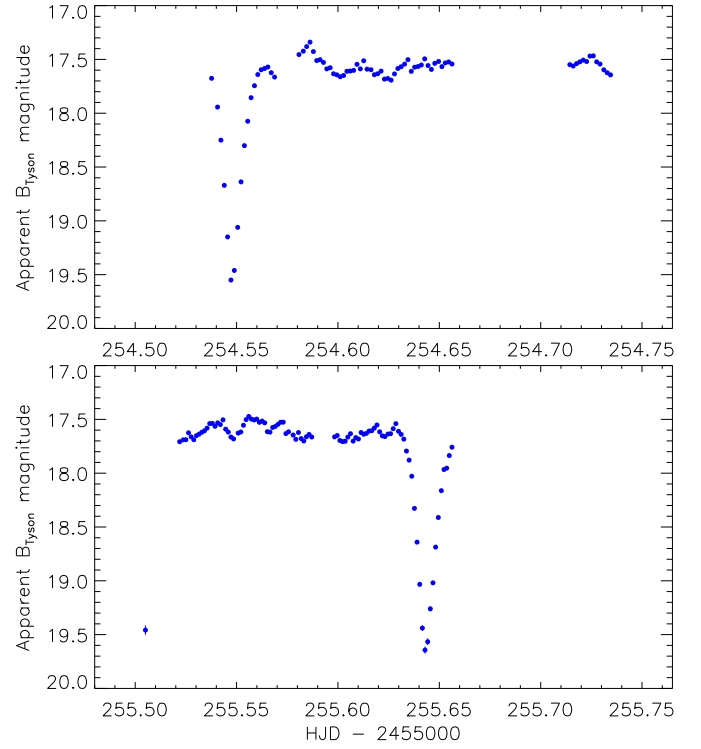
References. (1) Southworth et al. (2010); (2) This work; (3) Southworth et al. (2009a).

eclipse, before an unfortunate gap in observations for telescope maintenance. This single datapoint allows the orbital period of SDSS J0756 to be determined without cycle-count ambiguities, resulting in the ephemeris:

$$\text{Min I (HJD)} = 2455254.5481(1) + 0.136913(18) \times E$$

where E is the cycle count and the bracketed numbers represent the uncertainty in the last digit of the preceding number. This measurement corresponds to an orbital period of $P_{\text{orb}} = 197.154 \pm 0.025$ min, which puts SDSS J0756 beyond the 2–3 hr period gap seen in the period distribution of CVs, and right into the 3–4 hr period interval where most SW Sex stars are found. Its light curve is very similar to that of SDSS J075443.01+500729.2, an eclipsing SW Sex star with a period of 206.0 min (Southworth et al. 2007b).

The eclipsing nature of SDSS J0756 was first announced by Southworth et al. (2012). A detailed photometric and spectroscopic study of this object was presented by Tovmassian et al.

**Fig. 2.** The light curves of SDSS J0756. The errorbars are mostly smaller than the point sizes.

(2014) whilst the current work was nearing completion. Their orbital period measurement is in good agreement with our own.

3.2. SDSS J093537.46+161950.8

SDSS J0935 was found to be a CV by Szkody et al. (2009) due to the presence of Balmer and He I emission lines in its SDSS spectrum. He II $\lambda 4686$ emission is strong, leading Szkody et al. to suggest that it may contain a magnetic white dwarf, or alternatively be an old nova. We detected eclipses immediately on pointing the NTT towards it (Fig. 3). Three consecutive eclipses were seen on the night of 2010/02/24, followed by two more on subsequent nights. Fitting a straight line to the five times of mid-eclipse (Table 3) yields the orbital ephemeris:

$$\text{Min I (HJD)} = 2455251.56661(21) + 0.0640591(53) \times E$$

This measurement corresponds to $P_{\text{orb}} = 92.245 \pm 0.008$ min: SDSS J0935 is a good candidate for follow-up high-speed photometry (see fig. 2 of Littlefair et al. 2008).

The 2010/02/24 light curve of SDSS J0935 presents a notable post-eclipse maximum. Such humps in the light curves of CVs are usually explained as continuum radiation from the impact site of the gas stream from the secondary star on the accretion disc. However, such origin should leave its footprint at orbital phase ~ 0.8 , i.e. just before the eclipse. A post-eclipse maximum was observed during outburst for the long-period (0.2096 d) dwarf nova SDSS J081610.84+453010.2 (Shears et al. 2011), but there the brightness subsequently declines smoothly towards eclipse, leaving the impression of a broad obscuration feature rather than an isolated maximum. Bailey et al. (1988) found post-eclipse humps in the magnetic CV WW Hor, but in that case they are clearly related to cyclotron emission, and the spectrum of SDSS J0935 does not sug-

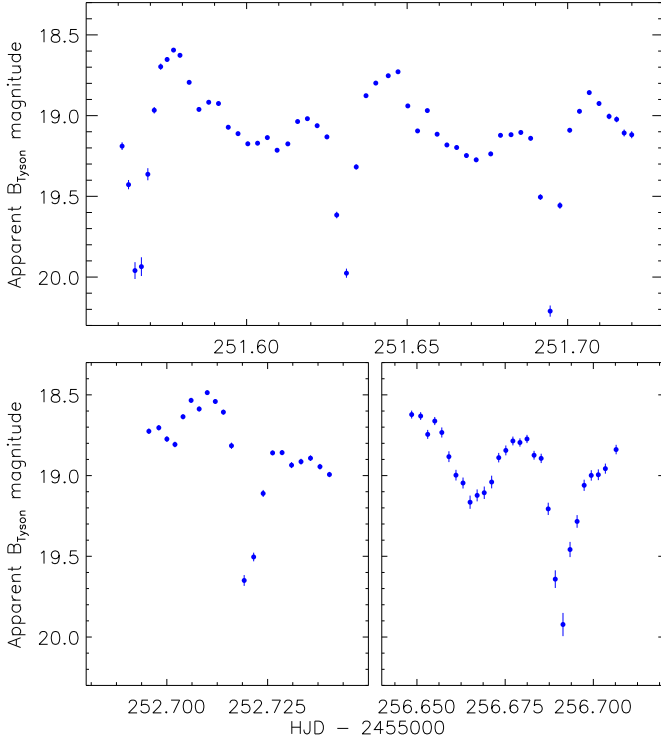


Fig. 3. The light curves of SDSS J0935.

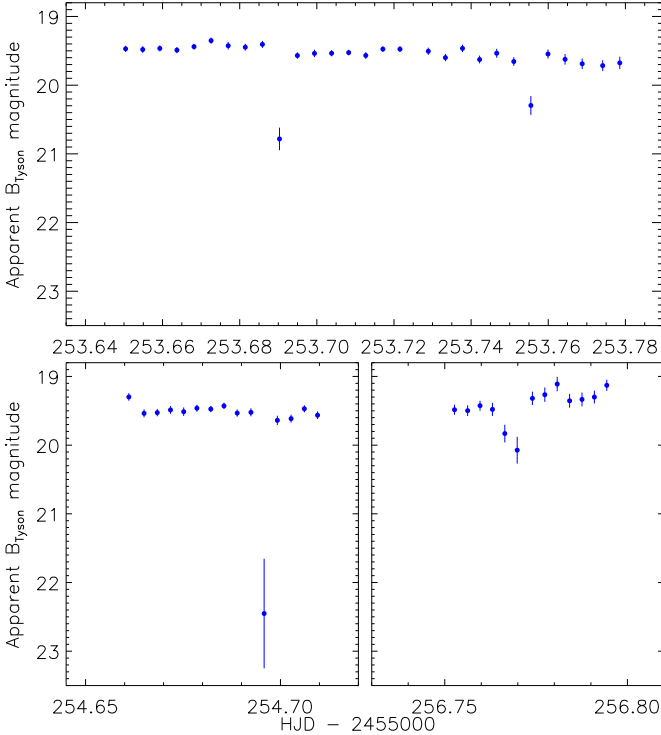


Fig. 4. The light curves of SDSS J1057.

gest the presence of a strongly magnetic white dwarf. The hump in WW Hor is unstable, and changes phase from ~ 0.2 to ~ 0.8 between nights.

It therefore appears that post-eclipse hump in SDSS J0935 follows a different period to the orbital period, suggesting a re-

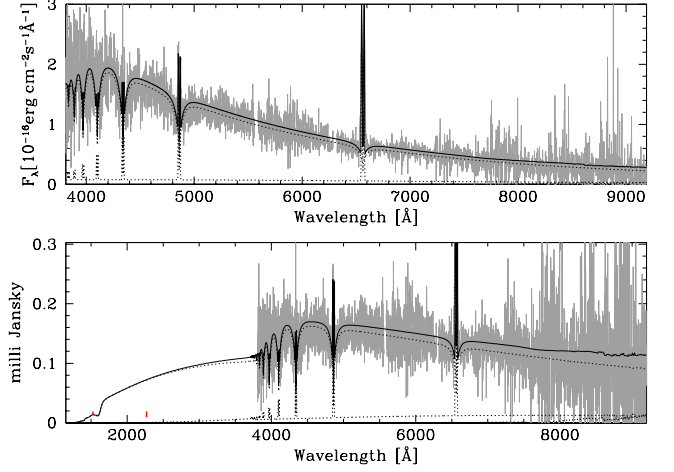


Fig. 5. Three-component model of the SDSS spectrum of SDSS J1057. The three components are a white dwarf with a temperature of 10 500 K, and surface gravity of $\log g = 8.0$ (c.g.s.); an isothermal and isobaric hydrogen slab, and an L5 companion star, all scaled to a distance of $d = 210$ pc. The two red points represent data from the GALEX satellite.

lation to superhumps. But these should occur exclusively in superoutburst for short period CVs, and the object appears to have been in quiescence during our observations. Still, we note that the spectrum by Szkody et al. (2009) presents a rather steep blue continuum and broad, but weak, Balmer emission compared to other short-period dwarf novae. SDSS J0935 is certainly an object worthy of further investigation.

3.3. SDSS J105754.25+275947.5

SDSS J1057 is another object identified as a CV by Szkody et al. (2009), who suggested that it might be eclipsing due to the double-peaked nature of its H α emission line (Fig. 1). Here we present the discovery that it is indeed an eclipsing system (Fig. 4) and the first measurement of its orbital period. We observed two consecutive eclipses on the night of 2010/02/26 and two on later nights. The eclipses are short and deep, and are entirely encompassed by one datapoint in our light curves. We therefore take the midpoints of those datapoints as the times of mid-eclipse, which results in the ephemeris:

$$\text{Min I(HJD)} = 2455253.6913(11) + 0.062807(43) \times E$$

with $P_{\text{orb}} = 90.44 \pm 0.06$ min. There is an alternative orbital ephemeris with different cycle counts and $P_{\text{orb}} = 96.40 \pm 0.07$ min, but this can be rejected from inspection of the residuals of the ephemeris fit and of the light curve plotted against orbital phase. Further observations, at a higher time resolution, could provide an independent confirmation of this result.

The light curve of SDSS J1057 is rather flat outside eclipse; this is most discernible by comparison to SDSS J0935 and CSS J1325. Most short-period CVs have a pronounced ‘orbital hump’ immediately before eclipse, caused by the bright spot on the edge of the accretion disc rotating into view. The faintness of the bright spot in SDSS J1057 suggests that this system was in a state of very low accretion at the time of our observations. Despite this, there is no sign of the secondary star in the SDSS spectrum (Fig. 1) even though the white dwarf primary is clearly

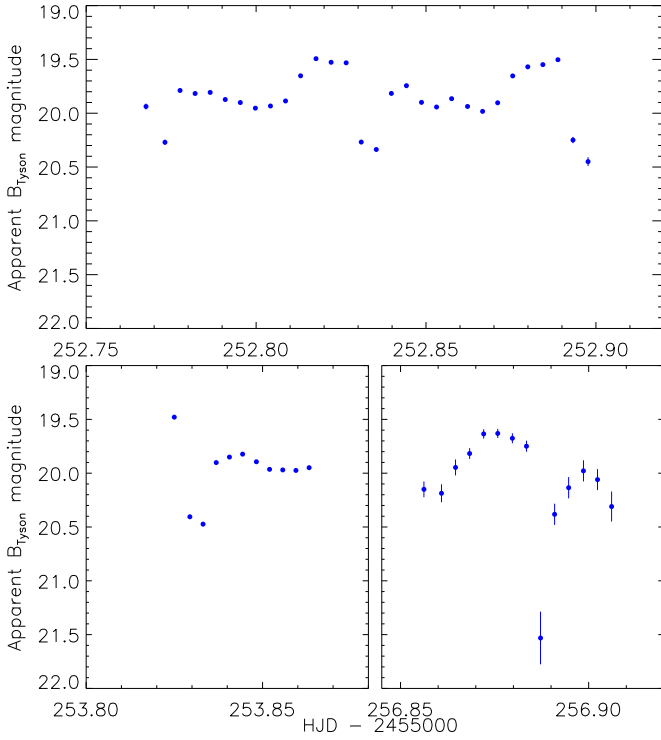


Fig. 6. The light curves of CSS J1325.

visible. SDSS J1057 is a good candidate for a period-bounce system, and deserves more detailed study.

We have analysed the spectral energy distribution of SDSS J1057 using the SDSS spectrum and GALEX fluxes (Morrissey et al. 2007). We find a decent fit to these data using the model of Gänsicke et al. (2006) with a white dwarf effective temperature of 10 500 K, an L5 secondary star, and an accretion disc of temperature 5800 K, all at a distance of 210 pc (Fig. 5). The GALEX near-ultraviolet flux is much lower than predicted, and may have been taken during eclipse. The low white dwarf temperature and late secondary-star spectral type are consistent with SDSS J1057 being a post-bounce system with a very low accretion rate.

3.4. CSS J132536+210037

CSS J1325 was detected as a probable dwarf nova by the *Catalina Real Time Transient Survey*⁵ (CRTS; Drake et al. 2009), based on a light curve in which the star was normally around magnitude 20 but twice brightened by at least 1.5 mag. It was included in a study of dwarf novae by Wils et al. (2010), who also noticed that its SDSS *ugriz* apparent magnitudes returned highly unusual colour indices. This was interpreted as the possible onset of eclipse during the SDSS photometric observations, which are taken in the order *riuzg* and with individual integration times of 54.1 s.

We therefore targeted CSS J1325 as a possible eclipsing CV, obtaining immediate confirmation. The first two brightness measurements we obtained of this object differed by 0.34 mag. Three consecutive eclipses were observed on the night of 2010/02/25,

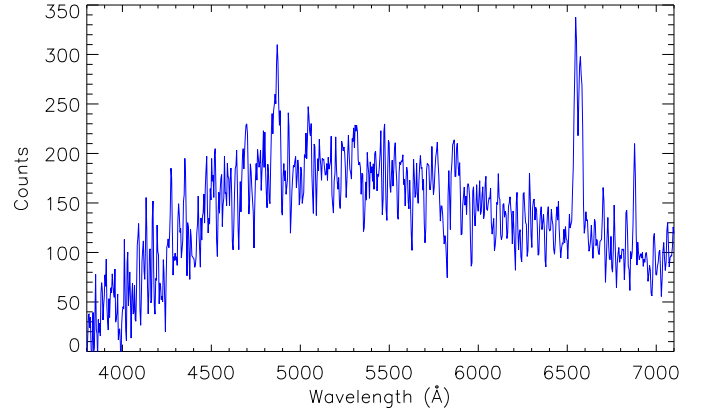


Fig. 7. Spectrum of CSS J1325 represented as counts per wavelength increment. The spectrum has been smoothed with a Savitsky-Golay filter to aid in the identification of spectral lines.

and two more were measured on later nights in our NTT run. We find the orbital ephemeris:

$$\text{Min I}(\text{HJD}) = 2455252.833222(85) + 0.06223756(61) \times E$$

which gives $P_{\text{orb}} = 89.821 \pm 0.009$ min. A spectrum of CSS J1325 was not obtained by the SDSS, as its eclipse-affected *ugriz* apparent magnitudes place it outside the high-priority regions in colour space. However, its eclipsing nature makes CSS J1325 well suited to further observations aimed at measuring its physical properties.

3.4.1. A spectrum of CSS J1325

Whilst observing we took the opportunity to obtain an identification spectrum of CSS J1325 (Fig. 7). For these observations EFOSC was equipped with grism #11, yielding a reciprocal dispersion of 2.0 Å px^{-1} and a resolution of 17 Å . Three exposures of 900 s each were obtained, wavelength-calibrated with a helium-argon arc line observation, and combined into one spectrum. Data reduction was performed with the PAMELA and MOLLY packages (Marsh 1989) in the same way as in previous papers in this series (Southworth et al. 2008a,b).

The final spectrum of CSS J1325 (Fig. 7) is rather noisy, due to the faintness of the target star and the relatively poor seeing, but clearly shows moderately weak emission lines at $H\alpha$ and $H\beta$. The $H\alpha$ emission is double-peaked, a common feature of the spectra of eclipsing CVs (e.g. SDSS J1057 in Fig. 1). Based on the above observations, CSS J1325 can be classified as a CV which shows both eclipses and dwarf nova outbursts.

4. New orbital ephemerides for four known eclipsing cataclysmic variables

4.1. SDSS J075059.97+141150.1

SDSS J0750 was identified as a CV by Szkody et al. (2007), on the basis of its SDSS spectrum. It was discovered to be eclipsing by Southworth et al. (2010), who measured an orbital period of 134.1564 ± 0.0008 min. We have observed one further eclipse of this system (Fig. 8), allowing the uncertainty in the orbital period to be lowered by an order of magnitude. We revise the linear orbital ephemeris to:

$$\text{Min I}(\text{HJD}) = 2454879.435968(69) + 0.093165454(30) \times E$$

⁵ <http://crt.s.caltech.edu/>

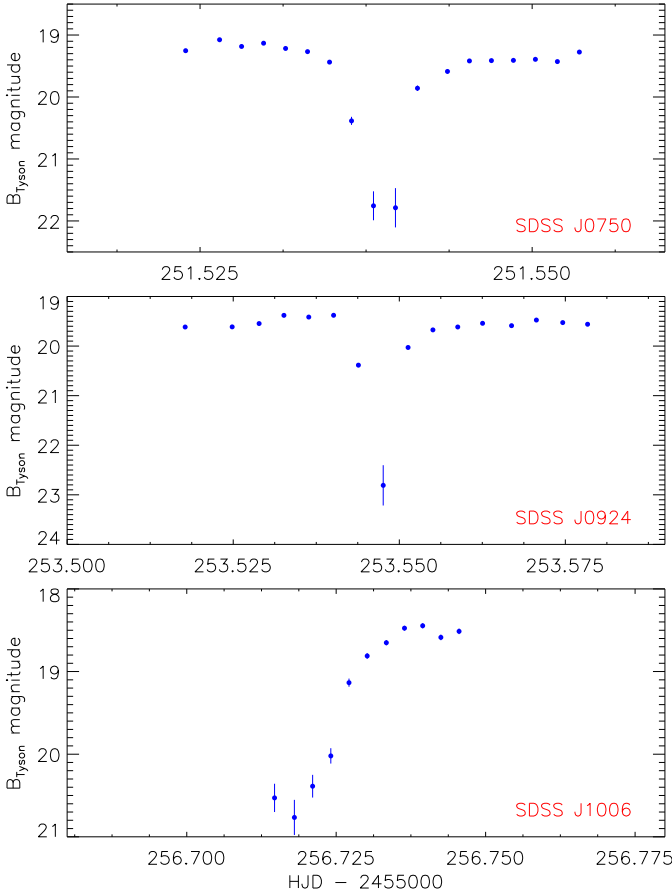


Fig. 8. The light curves of the known eclipsing CVs SDSS J0750, SDSS J0924 and SDSS J1006, obtained in order to improve their orbital ephemeris.

corresponding to a period of 134.15825 ± 0.00004 min. The cycle count over the intervening 13 months is unambiguous: the nearest alternative period differs by 45σ from the original value found by Southworth et al. (2010).

4.2. SDSS J092444.48+080150.9

SDSS J0924 (also named HULeo⁶) was identified by Szkody et al. (2005) as a possible magnetic CV from an SDSS spectrum which shows strong and narrow Balmer and He II emission and hints of the secondary star towards the red. Southworth et al. (2010) found it to be eclipsing, with no obvious sign of an accretion disc, and measured its orbital period to be 131.2432 ± 0.0014 min. We have obtained a light curve covering one additional eclipse (Fig. 8), which was detected in only three datapoints so is very undersampled. We take the midpoint of the middle datapoint as the derived eclipse time, and half the exposure time as its uncertainty. The resulting ephemeris is:

$$\text{Min I (HJD)} = 2454879.50461(11) + 0.09114108(31) \times E$$

Cycle count errors can be rejected at the 24σ level.

⁶ *Simbad* erroneously lists SDSS J0924 (HULeo) as a detached eclipsing binary.

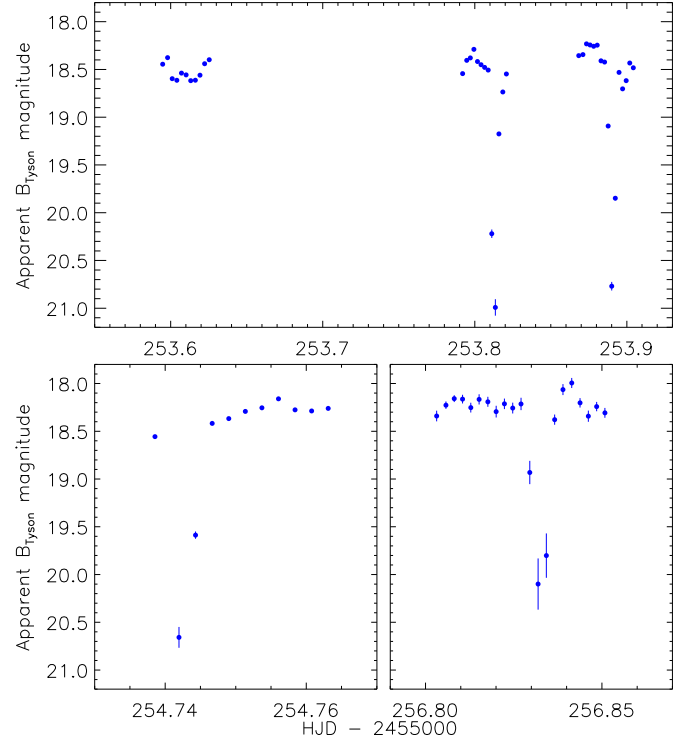


Fig. 9. The light curves of CSS J1126.

4.3. SDSS J100658.40+233724.4

SDSS J1006 was originally identified as a CV by Szkody et al. (2007), from an SDSS spectrum showing strong and wide Balmer emission lines. Southworth et al. (2009a) obtained extensive photometry and spectroscopy, from which they measured the orbital period of the system (267.71507 ± 0.00060 min) and the masses and radii of the component stars. We obtained a light curve of part of one additional eclipse (Fig. 8), doubling the temporal coverage of the photometric observations of this system. We find an improved orbital ephemeris of:

$$\text{Min I (HJD)} = 2454540.57962(16) + 0.18591331(12) \times E$$

SDSS J1006 is a long-period CV with $P_{\text{orb}} = 267.71516 \pm 0.00017$ min.

4.4. CSS J112634–100210

CSS J1126 was identified as an eclipsing CV from photometric observations taken by the CRTS. A dwarf nova outburst of amplitude 3 mag is also noticeable in these data (Drake et al. 2008). A subsequent spectrum confirmed the CV classification and revealed a ‘blue continuum with numerous H and He lines in emission’ (Djorgovski et al. 2008). CSS J1126 is positioned in an area of sky which was not covered in the SDSS spectroscopic observations, so does not have an SDSS spectrum.

We observed this object with the NTT in order to confirm its eclipsing nature and provide the first measurement of its orbital period. Two eclipses were observed in three short light curves taken on the night of 2010/02/26, and two more eclipses were targeted on subsequent nights. From the measured times of mid-eclipse we find the orbital ephemeris:

$$\text{Min I (HJD)} = 2455253.812683(86) + 0.0774466(34) \times E$$

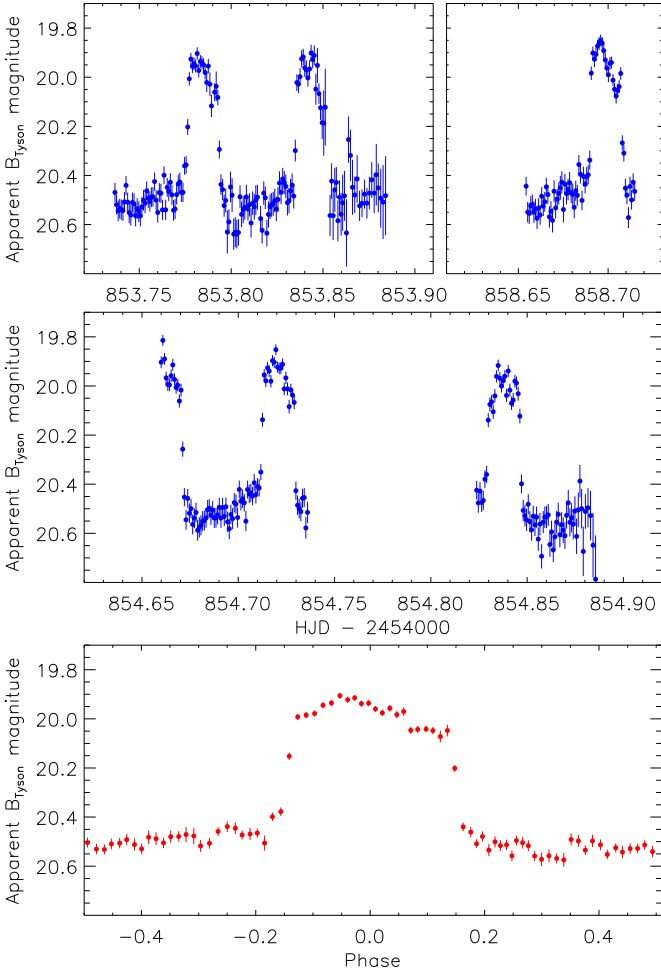


Fig. 10. The light curves of SDSS J0921 (upper panels). The lowest panel shows the photometric measurements as a function of orbital phase and binned by a factor of 5.

Table 4. Times of mid-brightening measured from our light curves of SDSS J0921.

Object	Time of mid-brightening (HJD - 2400000)	Cycle	Residual (d)
SDSS J0921	54853.7847 \pm 0.0002	0.0	-0.00014
SDSS J0921	54853.8435 \pm 0.0004	1.0	0.00016
SDSS J0921	54854.7208 \pm 0.0002	16.0	-0.00004
SDSS J0921	54854.8380 \pm 0.0002	18.0	0.00016
SDSS J0921	54858.6988 \pm 0.0002	84.0	-0.00003

which corresponds to $P_{\text{orb}} = 111.523 \pm 0.005$ min. The light curve of CSS J1126 is similar to that of SDSS J1057, in that it is fairly flat outside eclipse. This implies that either the accretion rate was low or the bright spot was optically thick at the time of our observations.

5. Three magnetic cataclysmic variables

5.1. SDSS J092122.84+203857.1

SDSS J0921 was discovered to be a magnetic CV of polar type by Schmidt et al. (2008). Its SDSS spectrum (Fig. 1) contains four clear cyclotron humps, which indicate that the white dwarf has a magnetic field strength of 32 MG. The follow-

up spectropolarimetric observations obtained by Schmidt et al. (2008) show variability in both polarisation and flux distribution. Schmidt et al. interpreted their observations as evidence of a positively polarised accretion region visible at all times, plus a negatively polarised region visible for only a small fraction of each orbital period. The orbital period of the system was only constrained to be greater than approximately 1.5 hr.

We observed SDSS J0921 on three nights in 2009 January, at which time it displayed brightenings of 0.6 mag amplitude, occurring every 84 min and lasting roughly 30 min (Fig. 10). These brightenings are telltale signs of an accretion column near the surface of the magnetic white dwarf rotating into and out of view. In order to find the orbital ephemeris we determined the mid-points of these brightenings in exactly the same way as eclipses were measured for the systems above. The mid-points are given in Table 4, and result in the ephemeris:

$$\text{Max(HJD)} = 2454853.78484(13) + 0.0584999(30) \times E$$

Under the reasonable assumption that these brightening represent the orbital period of the system, we find $P_{\text{orb}} = 84.240 \pm 0.004$ min.

The photometric variations of SDSS J0921 are strikingly similar to those of EU Cnc (Gilliland et al. 1991; Nair et al. 2005) and VV Pup (Warner & Nather 1972). These two objects are AM Her-type magnetic CVs, with orbital periods of 125.5 and 100.4 min, respectively. The variability in their light curves is thought to be due to cyclotron emission from accretion columns above the magnetic poles of the white dwarf. In the case of VV Pup, spectroscopic observations have verified that the photometric period coincides with the orbital period (e.g. Schneider & Young 1980), supporting our assertion above. Such observations have not been secured for EU Cnc.

5.2. SDSS J132411.57+032050.4

SDSS J1324 (also named PZ Vir) is a faint magnetic CV discovered by Szkody et al. (2003) from its SDSS spectrum, which shows a very faint object ($g = 23.3$) with a large flux excess around 5600 Å. From this and two other fainter cyclotron features, Szkody et al. (2003) inferred that the white dwarf has a magnetic field strength of 63 MG. They also obtained a short light curve which showed variability at a period of roughly 2.6 hr, and spectropolarimetry which demonstrated that the cyclotron feature is highly circularly polarised. SDSS J1324 has a very low accretion rate in which the accretion energy is not dissipated in a shock but instead is efficiently converted into optical cyclotron emission at and below the surface of the white dwarf (labelled the ‘bombardment scenario’). Szkody et al. (2004) obtained an XMM-Newton observation of the system which showed it to be a very weak X-ray source, in agreement with this scenario. Schmidt et al. (2005) presented spectropolarimetry of SDSS J1324 from which they measured a spectroscopic orbital period of 157 ± 14 min and deduced that the spin frequency of the white dwarf is locked to the orbital frequency.

We observed SDSS J1324 on three consecutive nights in 2009 January, at which time it was showing clear periodic variability (Fig. 11). Periodograms were calculated from the light curves using the Scargle (1982) method, analysis of variance (Schwarzenberg-Czerny 1989) and orthogonal polynomial (Schwarzenberg-Czerny 1996) approaches, as implemented within the TSA⁷ context in MIDAS. In all cases the best period was

⁷ <http://www.eso.org/projects/esomidas/doc/user/98NOV/vol1b/node220.html>

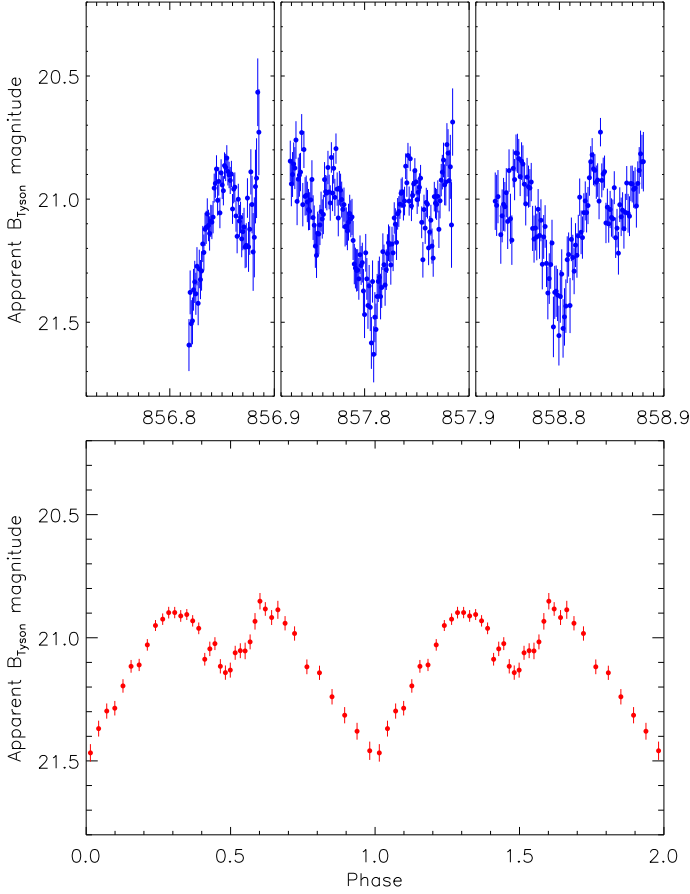


Fig. 11. The light curves of SDSS J1324 (upper panels). The lowest panel shows the photometric measurements as a function of phase and binned by a factor of 8. Two phases are reproduced for display purposes.

in the region of 159 min, and other peaks in the periodograms led to phased light curves with a much larger scatter. Taking into account the range of results found using the different periodogram methods, we arrive at a final period measurement of 158.72 ± 0.10 min.

The light curve phased using this period measurement is plotted in the lower panel of Fig. 11. Its morphology is notably reminiscent of the light curve of the prototypical polar AM Her presented by Szkody & Brownlee (1977). The variability is likely due to different degrees of cyclotron beaming towards Earth as the angle between the line of sight and the magnetic field axis changes over the orbit (Gänsicke et al. 2001). Ferrario et al. (2005) have studied the existing spectropolarimetric observations of SDSS J1324 and found good results with a model where the accretion energy is released relatively deep inside the white dwarf. The much improved accuracy of our period measurement for SDSS J1324 will help in the understanding of this candidate low-accretion-rate polar system (Schmidt et al. 2005).

5.3. SDSS J133309.19+143706.9

SDSS J1333 was found to be a magnetic CV by Schmidt et al. (2008), who measured an orbital period of 132 ± 6 min from spectroscopic velocity measurements of its H α emission line. Our observations, obtained from two telescopes, show obvious

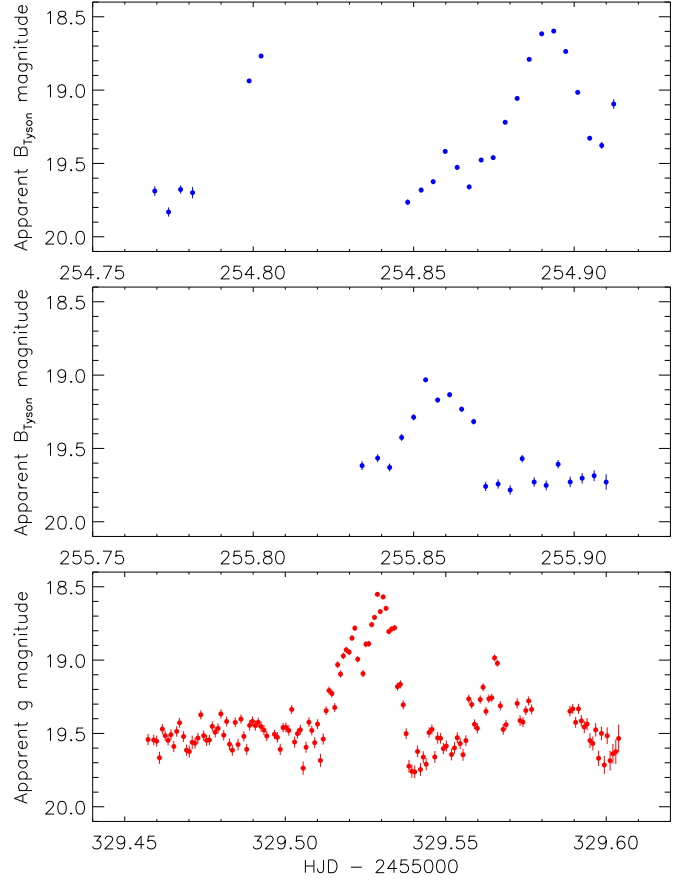


Fig. 12. Light curves of SDSS J1333. The upper two panels show data from the NTT and the lower panel data from the Calar Alto 3.5 m telescope.

variations in the optical brightness of this system (Fig. 12). Our data are consistent with an orbital period of 132 min but are insufficient to improve on this value. The light curve shape is reminiscent of the cyclotron-beaming brightenings displayed by SDSS J0921, suggesting that the orbital period of SDSS J1333 would be relatively easy to obtain from photometric observations with good coverage of all orbital phases.

6. The orbital period distribution of eclipsing CVs

The period distribution of CVs is an important observable quantity for comparison with theoretical population synthesis models (Patterson 1998; Knigge 2006; Gänsicke et al. 2009). CVs evolve from longer to shorter orbital periods through the loss of orbital angular momentum, before reaching a minimum period caused by changes in the structure of the secondary star and ‘bouncing’ back to longer periods. However, the observed orbital period distribution of CVs has persistently failed to match theoretical results (Downes et al. 2001; Ritter & Kolb 2003), which predict a large accumulation of objects at the minimum period due to the long evolutionary timescale there. Gänsicke et al. (2009) identified this ‘period spike’ for the first time, using the observed period distribution of the SDSS CVs. These authors demonstrated that the marked deficiency of short-period CVs could be an observational bias as these systems are intrinsically much fainter than longer-period systems.

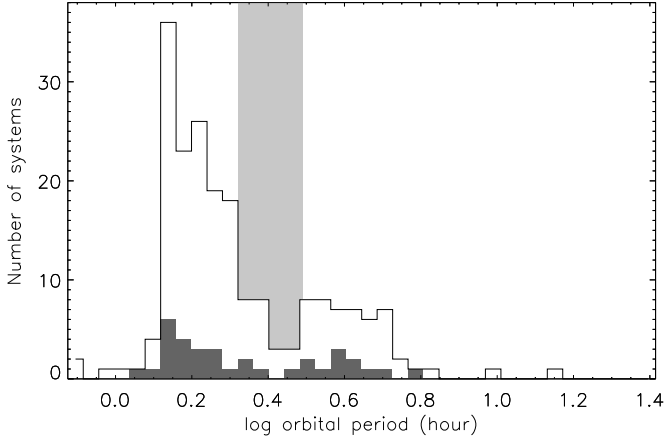


Fig. 13. The orbital period distribution of CVs identified by the SDSS (white histogram) and of the subset of these which are eclipsing (grey histogram). The light grey rectangle delineates the period gap at 2.1–3.1 hours. The periods have been collected into histogram bins which are of equal size in log space.

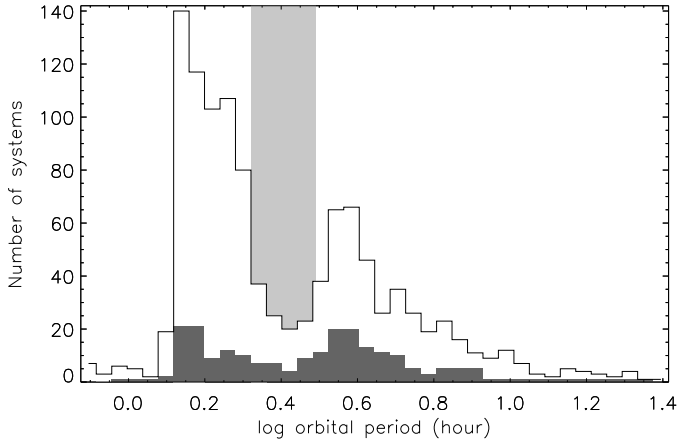


Fig. 14. As for Fig. 13 but for the RKCAt CVs.

Selection effects arise from the limiting magnitude and the method used to detect CVs (Gänsicke et al. 2009): identification via a blue colour (e.g. the Palomar-Green survey; Green et al. 1986) or low-resolution survey spectra (e.g. the Hamburg Quasar Survey; Hagen et al. 1995) tends to yield objects with a high accretion luminosity which are predominantly of longer orbital period. Medium-resolution survey spectroscopy (e.g. SDSS) yields samples of CVs which are comparatively unbiased, whereas CV discovery via outbursts is biased towards shorter-period objects (Uemura et al. 2010; Thorstensen & Skinner 2012; Woudt et al. 2012; see also Drake et al. 2014).

Selection effects also arise from the observational methods used to measure orbital periods. CVs do not give up their secrets easily, especially those which have high accretion rates. This leads to a bias against longer-period systems with higher accretion rates, as their periods are more difficult to measure and observers give them a lower priority for the same reason.

The study of eclipses is one of most straightforward ways to measure a CV orbital period, so has an important part to play in determining their period distribution. The likelihood of eclipses is a relatively flat function of orbital period (Warner

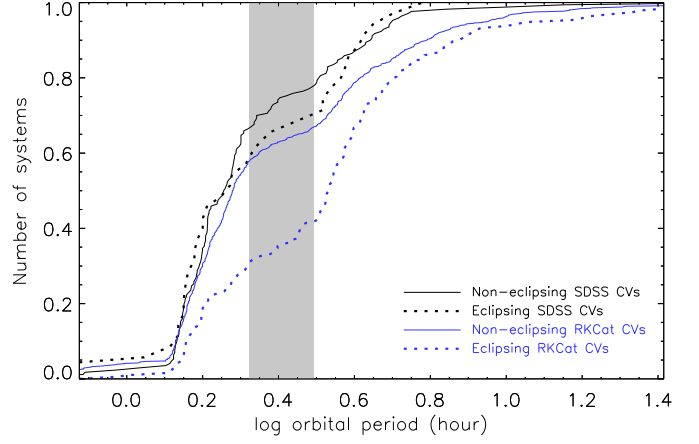


Fig. 15. Cumulative distribution of the orbital periods of SDSS and RKCAt CVs, both eclipsing and not eclipsing. The 2.1–3.1 hour period gap is shaded light grey.

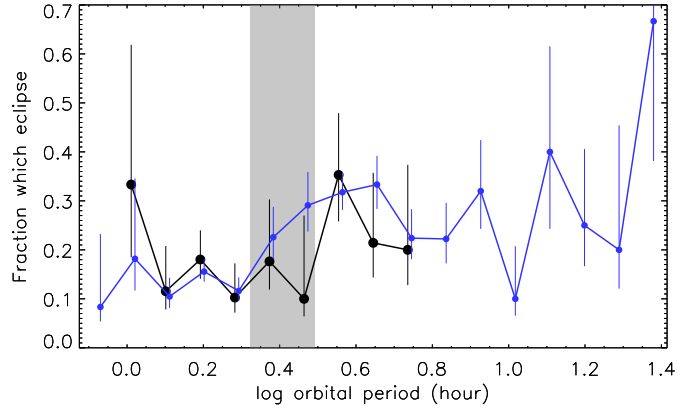


Fig. 16. The fraction of CVs which are eclipsing in the SDSS sample (black bold symbols) and in RKCAt (blue symbols). The samples have been combined into 17 bins for display purposes and 68.3% confidence intervals from binomial statistics are plotted. The RKCAt points are shifted by +0.01 in the abscissa to make them more visible

1995), but there are observational selection effects ?? favour of shorter periods (less telescope time is required per object) and against shorter periods (they are intrinsically fainter objects). Forthcoming large-scale sky surveys which are aimed at characterising the faint variable sky (e.g. LSST; Ivezić et al. 2008) will identify a large number of CVs. Most will be too faint for spectroscopic study with current facilities, so the investigation of these objects will rely heavily on the eclipsing ones.

Fig. 13 shows the orbital period distribution of all CVs identified from SDSS observations (data taken from Gänsicke et al. 2009 with updates). The prevalence of shorter-period systems is clear, and the fraction which are known to eclipse shows no significant trend with orbital period. Fig. 14 shows the known population of CVs according to version 7.20 (July 2013) of the Ritter & Kolb (2003) catalogue (hereafter RKCAt); note that this includes the SDSS CVs. A greater fraction of these objects have periods longer than the 2.1–3.1 hr period gap.

Fig. 15 represents these results as cumulative distributions, plotted for eclipsing and non-eclipsing CVs from the SDSS and the RKCAt sample. A slightly higher fraction of the SDSS CVs

Table 5. Summary of the orbital periods and CV classification obtained for the objects studied in this work.

Object	Period (min)	Notes
SDSS J0750	134.15825 ± 0.00004	Known eclipsing CV
SDSS J0756	197.154 ± 0.025	Known eclipsing CV
SDSS J0921	84.240 ± 0.004	Magnetic CV
SDSS J0924	131.2432 ± 0.0004	Known eclipsing CV
SDSS J0935	92.245 ± 0.008	New eclipsing CV
SDSS J1006	267.71516 ± 0.00017	Known eclipsing CV
SDSS J1057	90.44 ± 0.06	New eclipsing CV
CSS J1126	111.523 ± 0.005	First period measurement
SDSS J1324	158.72 ± 0.10	Magnetic CV
CSS J1325	89.821 ± 0.009	New eclipsing dwarf nova
SDSS J1333	(132 ± 6)	Magnetic CV

are shortward of the period gap, and the two distributions are similar to each other and to that of the RKCAt non-eclipsing CVs. The eclipsing RKCAt CVs, however, are predominantly longer-period: this is the only one of the four samples for which the majority of CVs are longward of the period gap. Possible explanations of this include that the eclipses in a significant number of the short-period RKCAt CVs have so far evaded detection or are not flagged as eclipsing in RKCAt, and that orbital period measurements in non-eclipsing long-period CVs are difficult so these objects are under-represented in RKCAt.

Fig. 16 shows the fraction of the SDSS and RKCAt samples which eclipse, as a function of orbital period. Few conclusions can be drawn for the SDSS sample, due to small-number statistics, but it is apparent that the eclipsing fraction does not have a strong dependence on period. The RKCAt sample, however, shows that a greater fraction of known longer-period CVs exhibit eclipses.

7. Summary

We present NTT/EFOSC2 time-series photometry of eleven CVs, eight of which show eclipses and three of which accommodate magnetic white dwarfs. Four of the targets were not previously known to be eclipsing, and for these plus a fifth object we provide the first measurement of their orbital periods (Table 5). These CVs are prime candidates for detailed follow-up observations of their eclipses, from which their physical properties can be measured to high precision.

The newly-discovered eclipsing systems include CSS J1325, which has an orbital period of 89.921 min, SDSS J1057 (90.44 min), SDSS J0935 (92.245 min) and CSS J1126 (111.523 min). We confirm the eclipsing nature of SDSS J0756 (197.154 min), which was recently discovered by Tovmassian et al. (2014). Along with SDSS J0750 (134.158 min) and the seven systems considered in Littlefair et al. (2008), they form a sequence which would allow the physical properties of short-period CVs to be empirically defined as a function of orbital period. We present the first spectrum of CSS J1325, which confirms its classification as an accreting binary system.

We also present photometry of three magnetic CVs and measure orbital periods for two of these, SDSS J0921 (84.240 min) and SDSS J1324 (158.72 min). The spectra and light curves of both are dominated by polarised emission arising from cyclotron radiation, and are strongly reminiscent of the magnetic CVs EU Cnc and AM Her, respectively. Finally, light curves of the

magnetic system SDSS J1333 were obtained which confirm its optical variability but do not yield a unique period measurement.

Five of the seven CVs for which we present the first orbital period measurements have periods shorter than the 2–3 hr gap observed in the general CV population (Whyte & Eggleton 1980). This is in line with previous results from our survey of SDSS CVs, where the general population of CVs is dominated by faint short-period systems (Gänsicke et al. 2009). The remaining two CVs are representatives of the AM Her and SW Sex classes of accreting binary systems, and have orbital periods within and beyond the period gap, respectively.

We construct the orbital period distributions of all SDSS CVs and of eclipsing SDSS CVs, finding that the fraction of eclipsing objects is not strongly dependent on orbital period. We perform this analysis for all CVs with a known orbital period in RKCAt. Whilst the fraction of eclipsing systems is comparable to the SDSS sample at shorter orbital periods, it rises towards longer periods. RKCAt is deficient in eclipsing CVs shortward of the period gap. The orbital period distribution of eclipsing CVs will be a key tracer of the population characteristics of CVs discovered in the future by deep sky surveys such as the LSST.

Acknowledgements. The reduced observational data presented in this work will be made available at the CDS (<http://cdsweb.u-strasbg.fr/>) and at <http://www.astro.keele.ac.uk/~jkt/>. We are grateful to Stuart Littlefair for suggesting CSS J1126 as a worthwhile target. JS acknowledges support from STFC in the form of an Advanced Fellowship. CMC and BTG acknowledge financial support from STFC in the form of grant number ST/F002599/1. The research leading to these results has received funding from the European Research Council under the European Union's Seventh Framework Programme (FP/2007-2013) / ERC Grant Agreement n. 320964 (WDTracer). BTG was supported in part by the UK's Science and Technology Facilities Council (ST/I001719/1). Based on observations made with ESO Telescopes at the La Silla Observatory under programme ID 084.D-0056. The following internet-based resources were used in research for this paper: the ESO Digitized Sky Survey; the NASA Astrophysics Data System; the SIMBAD database operated at CDS, Strasbourg, France; the arXiv scientific paper preprint service operated by Cornell University; and the AAVSO Variable Star Index.

References

- Araujo-Betancor, S., Gänsicke, B. T., Long, K. S., et al. 2005, *ApJ*, 622, 589
Bailey, J., Wickramasinghe, D. T., Hough, J. H., & Cropper, M. 1988, *MNRAS*, 234, 19P
Buzzoni, B., Delabre, B., Dekker, H., et al. 1984, *The Messenger*, 38, 9
Dillon, M., Gänsicke, B. T., Aungwerjwit, A., et al. 2008, *MNRAS*, 386, 1568
Djorgovski, S. G., Glikman, E., Mahabal, A., et al. 2008, *ATel*, 1416
Downes, R. A., Webbink, R. F., Shara, M. M., et al. 2001, *PASP*, 113, 764
Drake, A. J., Djorgovski, S. G., Mahabal, A., et al. 2009, *ApJ*, 696, 870
Drake, A. J., Gänsicke, B. T., Djorgovski, S. G., et al. 2014, *MNRAS*, in press, arXiv:1404.3732
Drake, A. J., Williams, R., Mahabal, A., et al. 2008, *ATel*, 1399
Ferrario, L., Wickramasinghe, D. T., & Schmidt, G. D. 2005, in *Astronomical Society of the Pacific Conference Series*, Vol. 330, *The Astrophysics of Cataclysmic Variables and Related Objects*, ed. J.-M. Hameury & J.-P. Lasota, 411–412
Gänsicke, B. T., Dillon, M., Southworth, J., et al. 2009, *MNRAS*, 397, 2170
Gänsicke, B. T., Fischer, A., Silvotti, R., & de Martino, D. 2001, *A&A*, 372, 557
Gänsicke, B. T., Rodríguez-Gil, P., Marsh, T. R., et al. 2006, *MNRAS*, 365, 969
Gilliland, R. L., Brown, T. M., Duncan, D. K., et al. 1991, *AJ*, 101, 541
Green, R. F., Schmidt, M., & Liebert, J. 1986, *ApJS*, 61, 305
Hagen, H.-J., Groote, D., Engels, D., & Reimers, D. 1995, *A&AS*, 111, 195
Hellier, C. 2001, *Cataclysmic Variable Stars: How and Why they Vary* (Springer-Praxis books in astronomy and space science, Springer Verlag, New York)
Horne, K., Wood, J. H., & Stiening, R. F. 1991, *ApJ*, 378, 271
Ivezić, Ž., Tyson, J. A., Acosta, E., & Others, M. 2008, arXiv:0805.2366
Jordi, K., Grebel, E. K., & Ammon, K. 2006, *A&A*, 460, 339
Knigge, C. 2006, *MNRAS*, 373, 484
Littlefair, S. P., Dhillon, V. S., Marsh, T. R., et al. 2008, *MNRAS*, 388, 1582
Littlefair, S. P., Dhillon, V. S., Marsh, T. R., et al. 2006, *Science*, 314, 1578
Marsh, T. R. 1989, *PASP*, 101, 1032
Morrissey, P., Conrow, T., Barlow, T. A., et al. 2007, *ApJS*, 173, 682
Nair, P. H., Kafka, S., Honeycutt, R. K., & Gilliland, R. L. 2005, *IBVS*, 5585

- Norton, A. J., Wynn, G. A., & Somerscales, R. V. 2004, *ApJ*, 614, 349
- Patterson, J. 1998, *PASP*, 110, 1132
- Ritter, H. & Kolb, U. 2003, *A&A*, 404, 301
- Rodríguez-Gil, P., Gänsicke, B. T., Hagen, H.-J., et al. 2007, *MNRAS*, 377, 1747
- Scargle, J. D. 1982, *ApJ*, 263, 835
- Schmidt, G. D., Smith, P. S., Szkody, P., & Anderson, S. F. 2008, *PASP*, 120, 160
- Schmidt, G. D., Szkody, P., Vanlandingham, K. M., et al. 2005, *ApJ*, 630, 1037
- Schneider, D. P. & Young, P. 1980, *ApJ*, 238, 946
- Schwarzenberg-Czerny, A. 1989, *MNRAS*, 241, 153
- Schwarzenberg-Czerny, A. 1996, *ApJ*, 460, L107
- Shears, J., Brady, S., Campbell, T., et al. 2011, *JBAA* accepted, *arXiv:1104.0104*
- Southworth, J., Copperwheat, C. M., Gänsicke, B., & Pyrzas, S. 2010, *A&A*, 510, A100
- Southworth, J., Gänsicke, B. T., & Breedt, E. 2012, in *IAU Symposium* 282, Cambridge University Press, Cambridge, UK., ed. M. T. Richards & I. Hubeny, 123–124
- Southworth, J., Gänsicke, B. T., Marsh, T. R., de Martino, D., & Aungwerojwit, A. 2007a, *MNRAS*, 378, 635
- Southworth, J., Gänsicke, B. T., Marsh, T. R., et al. 2006, *MNRAS*, 373, 687
- Southworth, J., Gänsicke, B. T., Marsh, T. R., et al. 2008a, *MNRAS*, 391, 591
- Southworth, J., Hickman, R. D. G., Marsh, T. R., et al. 2009a, *A&A*, 507, 929
- Southworth, J., Hinse, T. C., Burgdorf, M., et al. 2014, *MNRAS*, 444, 776
- Southworth, J., Hinse, T. C., Jørgensen, U. G., et al. 2009b, *MNRAS*, 396, 1023
- Southworth, J., Marsh, T. R., Gänsicke, B. T., et al. 2007b, *MNRAS*, 382, 1145
- Southworth, J., Townsley, D. M., & Gänsicke, B. T. 2008b, *MNRAS*, 388, 709
- Stetson, P. B. 1987, *PASP*, 99, 191
- Szkody, P., Anderson, S. F., Brooks, K., et al. 2011, *AJ*, 142, 181
- Szkody, P., Anderson, S. F., Hayden, M., et al. 2009, *AJ*, 137, 4011
- Szkody, P., Anderson, S. F., Schmidt, G., et al. 2003, *ApJ*, 583, 902
- Szkody, P. & Brownlee, D. E. 1977, *ApJ*, 212, L113
- Szkody, P., Henden, A., Fraser, O., et al. 2004, *AJ*, 128, 1882
- Szkody, P., Henden, A., Fraser, O. J., et al. 2005, *AJ*, 129, 2386
- Szkody, P., Henden, A., Mannikko, L., et al. 2007, *AJ*, 134, 185
- Thorstensen, J. R., Ringwald, F. A., Wade, R. A., Schmidt, G. D., & Norsworthy, J. E. 1991, *AJ*, 102, 272
- Thorstensen, J. R. & Skinner, J. N. 2012, *AJ*, 144, 81
- Tovmassian, G., Stephania Hernandez, M., González-Buitrago, D., Zharikov, S., & García-Díaz, M. T. 2014, *AJ*, 147, 68
- Uemura, M., Kato, T., Nogami, D., & Ohsugi, T. 2010, *PASJ*, 62, 613
- Warner, B. 1995, *Cataclysmic Variable Stars* (Cambridge Astrophysics Series, Cambridge University Press, Cambridge, UK)
- Warner, B. & Nather, R. E. 1972, *MNRAS*, 156, 305
- Webbink, R. F. & Wickramasinghe, D. T. 2002, *MNRAS*, 335, 1
- Whyte, C. A. & Eggleton, P. P. 1980, *MNRAS*, 190, 801
- Wils, P., Gänsicke, B. T., Drake, A. J., & Southworth, J. 2010, *MNRAS*, 402, 436
- Wood, J. H., Horne, K., Berriman, G., & Wade, R. A. 1989, *ApJ*, 341, 974
- Woudt, P. A., Warner, B., de Budé, D., et al. 2012, *MNRAS*, 421, 2414